IOPscience iopscience.iop.org

Home Search Collections Journals About Contact us My IOPscience

Induced magnetism at thin-film interfaces probed by means of x-ray magnetic circular dichroism

This article has been downloaded from IOPscience. Please scroll down to see the full text article.

2003 J. Phys.: Condens. Matter 15 S547

(http://iopscience.iop.org/0953-8984/15/5/309)

View the table of contents for this issue, or go to the journal homepage for more

Download details:
IP Address: 171.66.16.119
The article was downloaded on 19/05/2010 at 06:31

Please note that terms and conditions apply.

INSTITUTE OF PHYSICS PUBLISHING JOURNAL OF PHYSICS: CONDENSED MATTER

J. Phys.: Condens. Matter **15** (2003) S547–S559 PII: S0953-8984(03)54512-X

Induced magnetism at thin-film interfaces probed by means of x-ray magnetic circular dichroism

H Wende[1], A Scherz, F Wilhelm[2] and K Baberschke

Institut für Experimentalphysik, Freie Universität Berlin, Arnimallee 14, D-14195 Berlin–Dahlem, Germany

E-mail: babgroup@physik.fu-berlin.de (H Wende)

Received 9 October 2002
Published 27 January 2003
Online at stacks.iop.org/JPhysCM/15/S547

Abstract

We report on the induced magnetism at the interfaces of layered structures of 3d and 5d metals explored with the x-ray magnetic circular dichroism (XMCD) technique. The beginning as well as the end of the 5d series were analysed by investigating W/Fe and Ir/Fe superlattices. W is found to couple antiferromagnetically and Ir ferromagnetically to the Fe layers. The induced spin moment is oriented parallel to the induced orbital moment for the W as well as the Ir case. For the early 3d element vanadium, a thickness-dependent study was carried out for prototype Fe/V/Fe(110) trilayers to study the range of the polarization in vanadium. A short-range polarization was found, resolving inconsistencies between earlier theoretical and experimental works. Since the sum rule analysis usually used for the XMCD technique is not appropriate for the early 3d element vanadium, the experimental absorption fine structure and the magnetic dichroism are compared to *ab initio* calculations in order to obtain magnetic ground state properties.

1. Introduction

Layered structures consisting of ferromagnetic and non-magnetic metals are of technical as well as of fundamental interest. The investigation of layered magnetic structures is an active field of research because these structures present novel magnetic properties. Here, we discuss the important effects at the interfaces of multilayers and trilayer systems consisting of 3d and 5d transition metals, i.e. the induced magnetism at the interfaces due to hybridization and the orientation of the induced spin and orbital moments. In order to analyse the different contributions of the layers to the magnetism we use the element-specific x-ray absorption technique. This is very important for those systems where the induced total moment in

[1] Author to whom any correspondence should be addressed.
[2] Permanent address: European Synchrotron Radiation Facility (ESRF), BP 220, 38043 Grenoble, France.

 © 2003 IOP Publishing Ltd Printed in the UK

the non-magnetic layer is aligned antiparallel to the ferromagnetic layers. For those cases magnetometries such as vibrating-sample magnetometry (VSM) and superconducting quantum interference devices (SQUID) measure a reduced magnetization. These techniques cannot discern whether this reduction is due to a reduced magnetization in the ferromagnetic layer compared to bulk properties or whether the ferromagnetic layer shows the full magnetic moment and the reduction is due to an antiparallel-aligned induced moment at the interface of the non-magnetic layer. Furthermore, the x-ray magnetic circular dichroism (XMCD) technique allows the disentanglement of the total magnetic moment of the element investigated into its spin (μ_S) and orbital moment (μ_L), including the relative orientation of both. This is crucial when the g-factor is analysed; it is related to the spin and orbital moment by

$$\frac{\mu_L}{\mu_S} = \frac{g-2}{2}. \tag{1}$$

Ferromagnetic resonance (FMR) can determine the g-factor of the entire sample but a separation into the contributions of the individual layers is not possible (see the contributions by Lindner *et al* [33] and Pelzl *et al* [34]). This becomes especially important if $g < 2$ (spin μ_S and orbital moment μ_L antiparallel) for the material with the induced magnetism and if the ferromagnetic layer exhibits $g > 2$, i.e. $\vec{\mu}_S \parallel \vec{\mu}_L$. This demonstrates the need for an element-specific magnetometry for the analysis of the magnetism of layered structures. The x-ray absorption technique meets those demands: this spectroscopy measures the x-ray absorption coefficient $\mu(E)$ as a function of the incoming photon energy. Due to the different energy positions of the L-edges for each element, the analysis of $\mu(E)$ is element specific. Since the near-edge range is determined by the empty density of states, the spin and orbital moments and their relative orientation can be analysed using XMCD. In the past we used the element specificity of the XMCD technique to determine for instance the magnetic moments of the 3d ferromagnets Fe, Co, and Ni [1]. Here, this concept is applied to the 5d series (W and Ir) and to the early 3d element vanadium.

The paper is structured as follows. In section 2 we summarize how the spin and orbital moments and their relative orientation are determined by the application of the so-called sum rules. Then the induced magnetism in 5d elements is discussed in a systematic study for W and Ir in section 3. Since the application of the sum rules allows the analysis of the induced orbital and induced spin moments including the sign of both, the parallel or antiparallel alignment of μ_L and μ_S can be determined. Surprisingly, a breakdown of the third Hund's rule is found for the W case. In section 4 the question of the range of the polarization in the non-magnetic layer is investigated for prototype Fe/V/Fe trilayer systems. Conflicting results exist in the literature that either support long- or short-range polarization of V at the interface to Fe. Furthermore, the commonly used sum rules cannot be applied for the beginning of the 3d series. Therefore, the experimental spectra are compared to *ab initio* calculations.

2. Determination of spin and orbital moments using XMCD

In this section we briefly summarize how the spin and orbital moments can be determined from the XMCD L-edge spectra by applying the so-called sum rules. Details of this procedure can be found in various works, for instance [2–8]. Often the sum rules are applied in their integral form in order to calculate the orbital and spin moments μ_L and μ_S:

$$\mu_L^{3\mathrm{d}} = -\frac{2n_\mathrm{h}}{N}\int (\Delta\mu_{\mathrm{L}_3} + \Delta\mu_{\mathrm{L}_2})\,\mathrm{d}E, \tag{2}$$

$$\mu_S^{3\mathrm{d}} = -\frac{3n_\mathrm{h}}{N}\int (\Delta\mu_{\mathrm{L}_3} - 2\,\Delta\mu_{\mathrm{L}_2})\,\mathrm{d}E + 7\langle Tz\rangle, \tag{3}$$

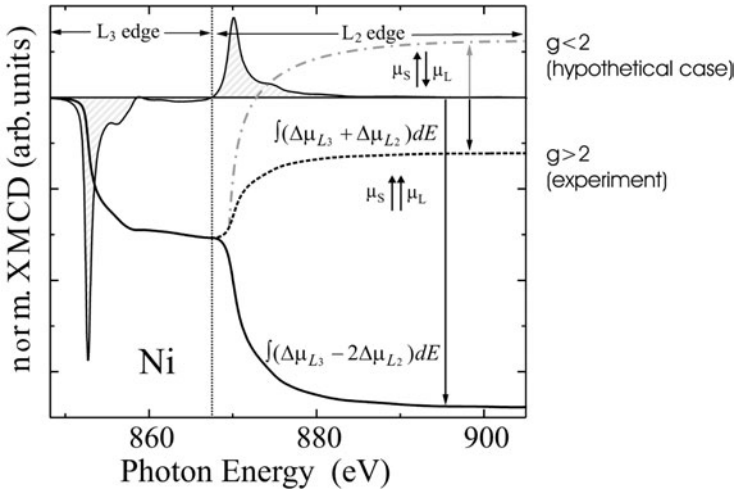

Figure 1. The XMCD difference for Ni and the XMCD integrals which are necessary for the application of the sum rules.

where $\Delta\mu_{L_3} = \mu^+_{L_3} - \mu^-_{L_3}$ refers to the XMCD difference of the x-ray absorption coefficients for right and left circularly polarized x-rays at the L_3 edge. N is the integral over the unpolarized absorption spectrum and n_h is the number of unoccupied d states (d holes). The application of the sum rules will now be discussed for a Ni XMCD spectrum given in figure 1. To determine the orbital moment μ_L the entire XMCD difference has to be integrated (marked area). This integral is given as the dashed curve. From the constant value marked by the arrow, μ_L can be calculated from equation (2). To determine the spin moment the L_2 signal must be subtracted from the L_3-edge one and hence the two contributions have to be separated. The corresponding integral is given by the solid curve and the constant value depicted by the larger arrow is used to calculate μ_S with equation (3). In the present paper we do not want to enter into the discussion about the quantitative applicability of the sum rules. A reasonably safe conclusion from the sum rules is the relative orientation of μ_L and μ_S: in the case of Ni given in figure 1 the negative signs for both integrals indicate the parallel alignment of the spin and orbital moments, corresponding to $g > 2$. In the case of $g < 2$ which is expected in the atomic picture for less than half-filled d-shells the integral of equation (2) would cross the zero line (the dot–dashed curve in figure 1). Hence, from the different signs of the integrals an antiparallel alignment of μ_L and μ_S would be concluded. This leads to the simple rule: if $\int(\Delta\mu_{L_3} + \Delta\mu_{L_2})\,dE$ crosses the zero line, spin and orbital moments are aligned antiparallel, and if there is no node, μ_L is parallel to μ_S. This procedure will now be discussed for the induced magnetism in Fe/W and Fe/Ir multilayers and for Fe/V/Fe trilayers.

3. Induced moments in 5d metals for Fe/W and Fe/Ir multilayers

The multilayers investigated here are prepared by electron-beam evaporation under ultrahigh-vacuum conditions. They were characterized by means of x-ray diffraction and transmission electron microscopy, revealing polycrystalline multilayer morphology with bcc (001) texture. The Fe thickness in each multilayer period is 10(1) Å and the W, Ir thicknesses are 5(1) Å, corresponding to about 3.0(5) monolayers (ML). Therefore the majority of the non-magnetic

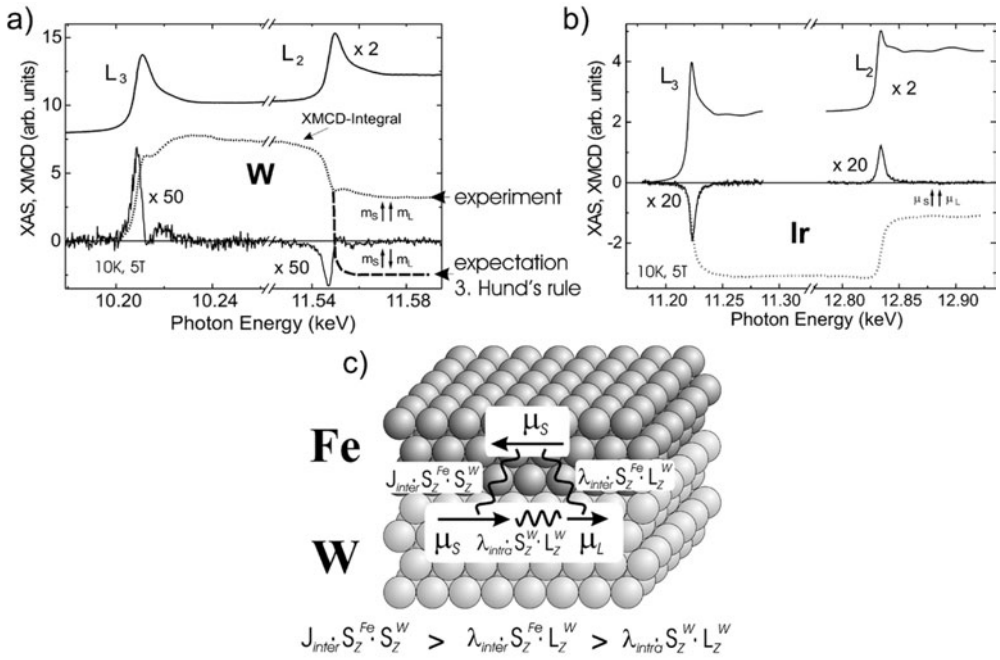

Figure 2. Normalized XAS and XMCD spectra at the $L_{3,2}$ edges of (a) W in Fe/W and (b) Ir in Fe/Ir multilayers [9]. For better illustration the XMCD spectra have been multiplied (W : $\times$50; Ir : $\times$20) and the XAS spectra have been shifted vertically. The XMCD integrals (dotted curves: measured; dashed curve: hypothetical) allow the analysis of the relative orientation of μ_L and μ_S. (c) A schematic representation of the Fe/W layers and the important interactions in a simple atomic model for the orientation of the Fe and W spin and orbital moments.

element is found at the interfaces. Details of the sample preparation can be found in [9, 10]. The XMCD data were measured in the hard-x-ray range at the beamline ID12A at the ESRF in a magnetic field of 5 T (normal to the film plane, parallel to the x-ray beam direction) at 10 K. The experimental results are given in figures 2(a) and (b) where the x-ray absorption coefficients for unpolarized radiation are presented together with the XMCD signals. These spectra reveal that small induced moments in W and Ir can indeed be found (please note the XMCD amplification factors $\times$50 for W and $\times$20 for Ir). Although the induced moments are relatively small (the analysis shows that the total induced moments for W and Ir are in the range of $\mu_{\rm tot} \approx 0.2\,\mu_{\rm B}$ [9]), the XMCD signals (figures 2(a) and (b) lower part) are clearly out of the noise. Even fine structures can be identified in the XMCD for W, which will be discussed later. First of all, one recognizes that the L_3-edge XMCD is positive for W and negative for Ir. Since the Fe XMCD at the L_3 edge in the soft-x-ray regime is negative, it can be concluded that the induced spin moment in tungsten is aligned antiparallel to Fe and the iridium spin moment is parallel to $\mu_S^{\rm Fe}$. This trend is found for all transition metal series. For a simple interpretation one can investigate the Bethe–Slater curve: the ratio of the inter-atomic distances to the radii of the incompletely filled d shells increases on moving from lower to larger filling. This leads to a change of the sign of the exchange integral J from negative (antiferromagnetic) to positive (ferromagnetic). Here, W represents the case of a less than half-filled 5d shell ($J < 0$) and Ir is more than half-filled ($J > 0$). It is important to note that 3d–5d hybridization changes the relative position of the majority and minority bands with respect to the Fermi level as found by theoretical calculations [11–13].

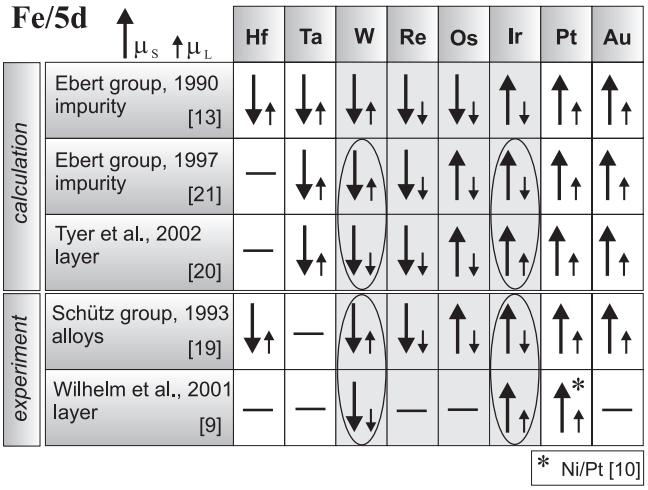

Figure 3. Schematic representation of the relative orientation of induced spin and orbital moments along the 5d series determined experimentally for alloys and layered structures. The experimental data are compared to theoretical calculations for the corresponding structures (impurities, layers).

Now we turn to the discussion of the integrals of the entire XMCD signal (dotted curves in figures 2(a) and (b)). For W as well as Ir the integrals do not have a node, indicating that the induced spin and orbital moments are aligned parallel for both cases ($g > 2$). This is surprising, since tungsten represents the case of a less than half-filled 5d shell in an atomic picture. It is clear that Hund's rules are in general only applicable for purely atomic systems but, on the other hand, in various solids the third Hund's rule holds. In contrast, the breakdown of the third Hund's rule was predicted theoretically for induced magnetism in uranium metals [14]. Here we give experimental evidence for the parallel orientation of the induced spin and orbital moments in tungsten in Fe/W multilayers. How can one understand the antiparallel orientation of μ_L^{W} and μ_S^{W} in a simplified atomic picture? In figure 2(c) we present the most important interactions:

(i) $J_{\mathrm{inter}} S_z^{\mathrm{Fe}} S_z^{\mathrm{W}}$

(ii) $\lambda_{\mathrm{intra}}^{\mathrm{W}} S_z^{\mathrm{W}} L_z^{\mathrm{W}}$

(iii) $\lambda_{\mathrm{inter}} S_z^{\mathrm{Fe}} L_z^{\mathrm{W}}$.

The largest one (i) is the direct *inter*-atomic exchange between the iron and tungsten spins. This interaction leads to the antiferromagnetic coupling between Fe and W. The *intra*-atomic spin–orbit coupling in tungsten (ii) would favour the antiparallel orientation of the induced μ_L^{W} and μ_S^{W} in W. But since μ_L^{W} and μ_S^{W} are experimentally found to be oriented parallel (see figure 2), there must be a larger interaction (iii) which we assign to an *inter*-atomic spin–orbit coupling between Fe and W. Also recent calculations for Fe layers on a W(110) substrate find that for these layered structures μ_L^{W} and μ_S^{W} are oriented parallel [15–17]. Hübner *et al* discuss a different mechanism for the parallel alignment of μ_L^{W} and μ_S^{W}: the effect could also be due to the large crystal field splitting of the 5d orbitals because the W 5d orbitals are affected strongly by the neighbouring atoms. The density of the 5d states is broadened to about 10 eV, which is twice the 3d DOS broadening for Fe [18].

The finding of the parallel orientation for μ_L^{W} and μ_S^{W} for the *layered* structures is remarkable, since an antiparallel alignment is found experimentally for the induced spin and orbital moments in W for alloys [19]. This can be seen in figure 3 where the relative

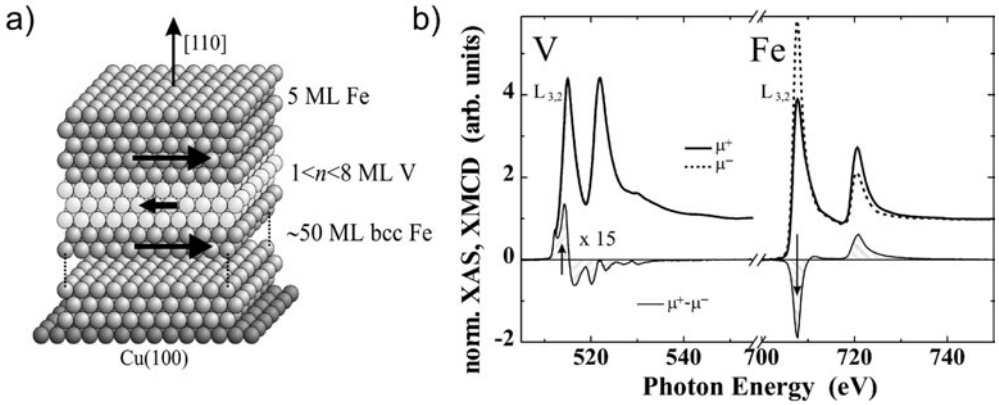

Figure 4. (a) A schematic representation of a prototype Fe/V/Fe(110) trilayer on a Cu(100) substrate. (b) The normalized XAS of right (solid curve) and left (dashed curve) circularly polarized light and the XMCD at the V and Fe $L_{3,2}$ edges of a $Fe/V_4/Fe(110)$ trilayer [26]. For better illustration, the V XMCD has been multiplied by 15.

orientation of the induced spin and orbital moments along the 5d elements at the interface to Fe is shown as determined experimentally for layered structures [9] and alloys [19]. A special case is the layered structure of Pt where an induced moment is determined at the interface to Ni [10] (marked with *). These results are compared to theoretical calculations for the relative orientation for layers [20] and impurities [13, 21]. The white fields mark those elements for which a clear parallel orientation of μ_L and μ_S is found (i.e. the heavy 5d elements Pt and Au), or a clear antiparallel alignment is determined (i.e. the light 5d elements Hf and Ta), respectively. The grey fields mark the intermediate area where both orientations can be found. Interestingly, a different behaviour of the relative orientation of μ_L and μ_S for the alloys compared to the layered structures can be seen experimentally for W and Ir (layers: parallel, alloys: antiparallel) as marked by the ellipses in the lower part of figure 3. These findings are supported by recent theoretical calculations for layers and impurities which also identify the same differences between alloys and layers as determined experimentally (marked by ellipses in the upper part of figure 3). This indicates that the induced magnetism in alloys is different from the one in multilayers because the bandstructure clearly differs for the two cases as we demonstrated recently [22]. These results illustrate the power of an element-specific technique such as the XMCD method. In the next section we want to analyse in detail for a 3d/3d interface how far away from the interface induced moments can be found in the non-magnetic layers.

4. Long- or short-range spin polarization of vanadium? Fe/V/Fe(110) trilayers as prototype systems

For Fe/V layered structures, conflicting results exist on the range of the polarization in vanadium. Theoretical works by Coehoorn predict a short-range polarization [23]. This means that the induced moment in V is basically located at the interface. In contrast, experimental works by Tomaz *et al* and Schwickert *et al* find that vanadium is in a 'transient ferromagnetic state' because induced moments in V are still found 4 ML away from the interface [24, 25]. In order to tackle these conflicts, we carried out a thickness-dependent XMCD study for prototype Fe/V/Fe(110) trilayer systems [26]. A schematic representation of a trilayer system is given in figure 4(a). In order to study the range of the polarization, the vanadium thicknesses were

varied in the range of 1–8 ML. The benefit of the preparation *in situ* is the controllable growth: on a Cu(001) single crystal a Fe buffer of 50 ML is prepared by e-beam evaporation. It is known that this buffer has bcc (110) structure [27, 28]. In order to reduce the surface roughness this Fe buffer was annealed to 400–450 K. Before depositing the V layer the sample was cooled down to 300 K in order to prevent interdiffusion at the interfaces. This is different from the usual multilayer preparation procedure where much higher sample temperatures of about 570 K [25] are needed because of the larger deposition rates using sputter deposition techniques. Then the V and the top Fe layers were grown at room temperature in our experiment. The XMCD data were recorded at the UE56/1-PGM beamline at BESSY II using the newly developed gap-scan mode. Details can be found in [26]. The experimental results for a $Fe/V_4/Fe(110)$ trilayer are shown in figure 4(b). Clearly the x-ray absorption coefficients for right and left circularly polarized x-rays $\mu^+(E)$ and $\mu^-(E)$ differ at the Fe $L_{3,2}$ edges, whereas hardly any difference can be made out by eye at the V $L_{3,2}$ edges. But because of the large photon flux and high degree of circular polarization, even this small V XMCD signal can be measured free of noise (please note the enlargement factor of 15 for the V XMCD). The positive XMCD signal at the V L_3 edge compared to the negative one at the corresponding Fe L_3 edge reveals an antiferromagnetic coupling between Fe and the induced V magnetic moments. This is similar to the Fe/W case discussed above, because V is nearly directly above W in the periodic table. Therefore the same arguments concerning the antiferromagnetic coupling given above hold, since V represents the case of a less than half-filled 3d shell. Also a clear asymmetry in the V XMCD at the L_3 edge can be detected which can be compared to the fine structure in the W L_3-edge XMCD in the hard-x-ray range (see figure 2). This asymmetry is due to the splitting of the initial core states which becomes prominent for the early 3d (V) and early 5d (W) elements [8, 22]. Now we turn to the XMCD results from the thickness-dependent study given in figure 5(a). The spectra are normalized to a constant edge jump so that the XMCD intensities are proportional to the V magnetic moment $\overline{\mu}_V$ averaged over the entire film. The samples were probed in magnetic remanence under 20° grazing incident light, and therefore, the Fe and V absorption spectra were corrected for self absorption effects [22]. Furthermore, the spectra were corrected so that they correspond to 100% degree of circular polarization and parallel alignment of the photon wavevector and the magnetization. We start with a discussion of the $Fe/V_2/Fe$ trilayer XMCD: a clear asymmetric signal can be seen at the L_3 edge. At about 520 eV the L_2-edge contribution sets in. This demonstrates that there is a strong overlap of the L_3- and L_2-edge contributions. This will become relevant for the question of the applicability of the sum rules for V discussed later. The lineshapes of the XMCD signal are very similar for all the thicknesses, since the XMCD differs mainly by a scaling factor. Comparing the results for the two layers of V to the four-layer XMCD, we find that the signal is nearly reduced by a factor two for the $Fe/V_4/Fe$ system. Because of the normalization, this shows that the two additional layers carry nearly no induced moment. The same trend is found for going from the $Fe/V_4/Fe$ to the $Fe/V_8/Fe$ system. This is a first indication that the induced moment in vanadium is basically located at the interface, revealing a short-range spin polarization of vanadium. Comparing $Fe/V_1/Fe$ to $Fe/V_2/Fe$, a strong increase of the signal is found for the one layer of V. This is due to the fact that the one layer is faced on two sides by the polarizing Fe layers. For a more detailed investigation of the thickness dependence, we discuss the product of the average V magnetic moment $\overline{\mu}_V$ and the V thickness n as a function of n, shown in figure 5(b). How these moments can be given in absolute units (μ_B/atom) will be discussed later. Here, we first focus on the relative changes. The values given in figure 5(b) are proportional to the (integral) XMCD intensity in figure 5(a) times the number of layers n. If one could indeed find V in a 'transient ferromagnetic state' as suggested by Schwickert *et al* [25], all the V layers would carry the same moment per atom. In this case one would find a

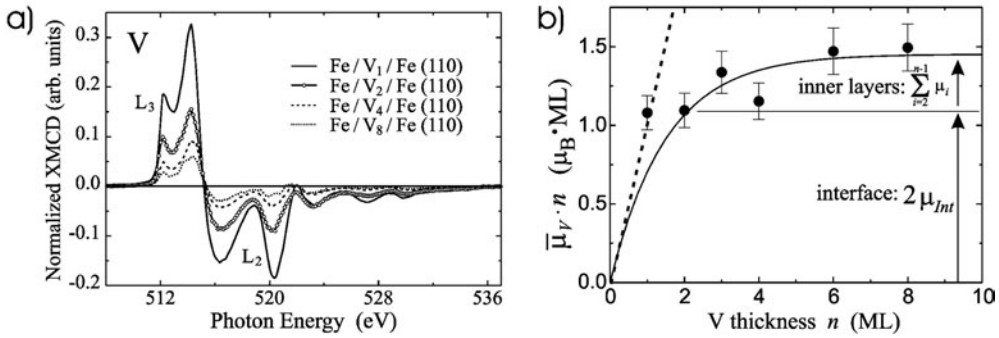

Figure 5. (a) The thickness dependence of the V $L_{3,2}$ XMCD for Fe/V_n/Fe(110) trilayers with $n = 1$, 2, 4, and 8 ML. (b) The average total V moment $\overline{\mu}_V$ times the V thickness n as a function of n. This product $\overline{\mu}_V n$ saturates above $n = 3$ ML, indicating a short-range polarization [26].

straight line with the slope of the constant vanadium moment as indicated by the dashed curve in figure 5(b) for the case of a (constant) moment of 1 μ_B. Our experimental results, on the other hand, exhibit a fast saturation of $\overline{\mu}_V n$ in the range of $n \approx 3$ ML. This demonstrates that the product of the averaged V moment and the number of layers is basically determined by the moments of the two interfaces μ_{Int} and a small contribution from the inner layers μ_i:

$$\overline{\mu}_V n = 2\mu_{Int} + \sum_{i=2}^{n-1} \mu_i. \tag{4}$$

From the fitting curve (solid curve in figure 5(b)) a V profile can be determined under the assumption that the induced moment only depends on the position of the layer relative to the interface layer. The result is given in figure 6: the shaded bars represent the induced V moments for the prototype Fe/V_n/Fe(110) trilayers with $n = 1$, 2, 3, 4, 6, 8. The profile shows that the induced V moments are basically located at the interface. A moment profile for the Fe layers cannot be determined because an averaged signal over the entire Fe buffer is investigated, which exhibits bulk-like properties. Therefore the Fe moment at the interface is presented in a schematic form only, in order to depict the antiparallel alignment between the Fe and the induced V moments. From the results in figures 5 and 6 obviously a short-range polarization can be concluded. The long-range polarization found in the earlier experimental works for Fe/V multilayers [25] might be an artefact, because in the analysis sharp interfaces were assumed although interdiffusion is very likely to happen at deposition temperatures of 570 K.

In figures 5 and 6 we give absolute magnetic moments for V. The question arises of how one can determine these moments, because a detailed analysis [22] reveals that the sum rules discussed in section 2 are not applicable to the early 3d element V. This failure is now discussed for a $Fe_{0.9}V_{0.1}$ alloy presented in figure 7. The alloy was prepared by simultaneous evaporation from high-purity Fe and V rods using a focused triple-e-beam evaporator at well defined fluxes. The experimental results for the polarization-averaged XAS and the corresponding XMCD are given by the solid curves in figure 7(a). The XAS data show that the intensity ratio of the absorption coefficient at the L_3 and L_2 edges—the so-called branching ratio—dramatically deviates from the ideal ratio of 2:1, being close to 1:1 for V. This demonstrates that strong core-hole correlation effects are present which make the application of the sum rules very questionable for vanadium [6], because spectral weight is transferred from the L_3 to the L_2 edge. This is because of the small spin–orbit splitting of the initial $2p_{3/2}$ and $2p_{1/2}$ states leading to a

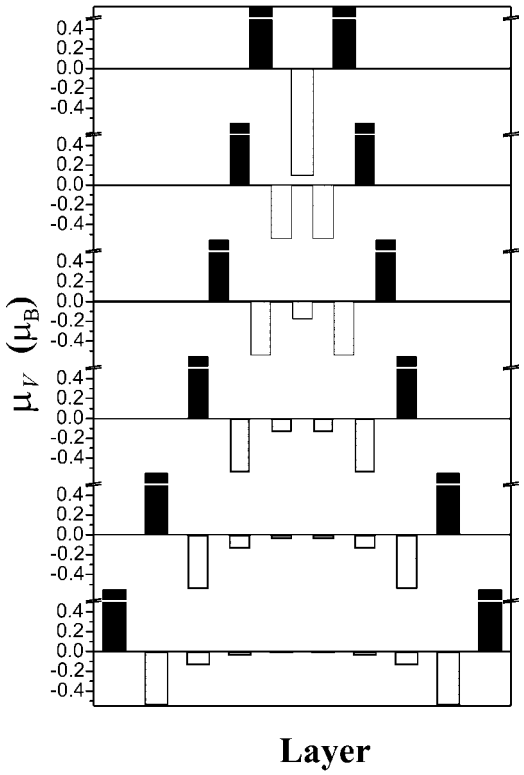

Figure 6. (a) The vanadium total magnetic moment profile (shaded bars) determined from the thickness-dependent study of the prototype $Fe/V_n/Fe(110)$ trilayers with $n = 1, 2, 3, 4, 6, 8$. The errors of the V moments are $\pm 15\%$. The Fe moments could not be determined in a layer-dependent fashion. Therefore the solid bars represent the Fe moment in schematic form in order to illustrate the antiparallel orientation of the Fe moment with respect to the induced V moment.

separation of the L_3 from L_2 edge by only about 7 eV. A strong overlap of the L_3 and L_2 XMCD contributions is the result, hindering the separation of the two contributions which is necessary for the spin moment determination as discussed in section 2 for equation (3). This becomes obvious when looking at the XMCD integrals given in figure 7(b). The analysis of the relative orientation of the induced spin with respect to the induced orbital moment is still relatively safe, since no separation of the edges has to be carried out. The integral being proportional to μ_L (dot–dashed curve) clearly shows a crossing of the zero line for V, whereas no node can be found for the corresponding Fe integral. This shows that the induced orbital moment is aligned antiparallel to the induced spin moment for V ($g^{\mathrm{V}} < 2$) whereas a parallel orientation of the spin and the orbital moment is found for Fe ($g^{\mathrm{Fe}} > 2$), following the expectations from the third Hund's rule. This is of great importance for the analysis of Fe/V multilayered systems (see Lindner *et al* [33]) because μ_L^{V} and μ_L^{Fe} are oriented parallel and therefore add, whereas μ_S^{V} and μ_S^{Fe} cancel each other. This leads to the determination of a larger g-factor in FMR measurements compared to element-specific measurements [29]. Despite the reliability of the discussion of the relative orientation of μ_S^{V} and μ_L^{V}, figure 7(b) demonstrates that the absolute determination of μ_S^{V} with the sum rules (solid curve) is very questionable, because it is not clear where the separation between the L_3-edge and the L_2-edge contributions has to be carried out. Although these difficulties are obvious, one can find applications of the sum rules for V in

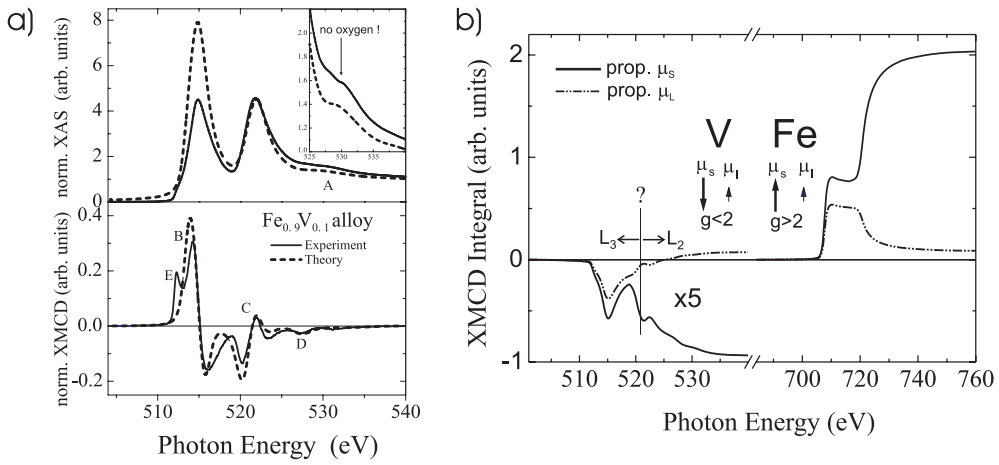

Figure 7. (a) Comparison of the experimental XAS and the corresponding XMCD at the V $L_{3,2}$ edges of a $Fe_{0.9}V_{0.1}$ alloy (solid curve) to theoretical calculations by Ebert *et al* [22] (dashed curve). (b) Experimental integrals (see equations (2) and (3)) at the V and Fe $L_{3,2}$ edges.

the literature, for instance by Sacchi *et al* [30] who used the x-ray resonant magnetic scattering technique which is related to XMCD. In order to circumvent this difficulty, a different approach has been used here: the experimental data are compared to theoretical calculations by Ebert and coworkers [22] using the fully relativistic spin-polarized Korringa–Kohn–Rostoker (SP-KKR) Green's function method. The results are given as dashed curves in figure 7(a). No core-hole correlation effects were included in the calculation, which explains the deviations in the XAS data at the L_3 edge. Nevertheless, a broad satellite feature A at about 532 eV (inset of figure 7(a)), which one could have falsely assigned to an oxygen contamination in the experiment, is well reproduced by the theory. This shows that the structure can be correlated with features in the V band structure, namely a van Hove singularity at the N point of the bcc Brillouin zone [22]. Looking at the XMCD, we find that nearly all fine structures in the experimental data can be reproduced by the theory: these are the asymmetric contributions from the L_3 edge (labelled B) and the L_2 edge (C) as well as the oscillatory fine structure (D). Only the pre-edge feature E is missed by the calculation. This indicates that the feature might originate from a multiplet structure. Furthermore, the theory provides the induced spin and orbital moments of $\mu_S^{\mathrm{V}}(\mathrm{theory}) = -1.01\ \mu_{\mathrm{B}}$ and $\mu_L^{\mathrm{V}}(\mathrm{theory}) = 0.020\ \mu_{\mathrm{B}}$ [22]. The negative sign indicates that the induced moment in V is oriented antiparallel to that in Fe. These values can be compared to apparent moments determined from the sum rule application to the experimental spectra of $\mu_S^{\mathrm{V}}(\mathrm{experiment,\ sum\ rule}) = -0.20\ \mu_{\mathrm{B}}$ and $\mu_L^{\mathrm{V}}(\mathrm{experiment,\ sum\ rule}) = 0.016\ \mu_{\mathrm{B}}$ [22] demonstrating that the sum rules are not applicable to the early 3d element vanadium, especially for the determination of the spin moment. But this difficulty can be overcome in the following way: the experimental XMCD data for the $Fe_{0.9}V_{0.1}$ alloy can be used as an experimental standard by pinpointing the spin and orbital moment for the alloy at the theoretical values. This provides correction factors for the spin and orbital sum rule with respect to this reference sample. The scaling procedure is reasonable since the lineshape of the thickness-dependent XMCD spectra is maintained for the trilayers and the alloy (see figure 5). Basically, only the amplitude of the dichroism changes, which is a good measure of the magnetic moment. The absolute moments given here are corrected for the T_z-term (see equation (3)) which is also obtained from the calculations [22]. The results for the

Table 1. Spin, orbital, and total moments for vanadium for the two samples in this work and a $(Fe_4/V_2)_{60}$ superlattice from [29] as deduced by scaling to the reference sample [22].

(μ_B/atom)	Alloy $Fe_{0.9}V_{0.1}$ (experimental standard)	Trilayer $Fe/V_2/Fe(110)$ (scaled)	Multilayer $(Fe_4/V_2)_{60}$ (scaled)
μ_S^{3d}	−1.01(15)	−0.57(8)	−0.93(15)
μ_L^{3d}	0.020(10)	0.025(12)	0.015(7)
μ_{tot}^{3d}	−0.99(15)	−0.54(8)	−0.91(15)

spin and orbital moments for the $Fe/V_2/Fe$ trilayer in comparison to a $(Fe_4/V_2)_{60}$ multilayer are given in table 1. Two points should be stressed here: it turns out that the total magnetic moment for the $(Fe_4/V_2)_{60}$ multilayer is $\mu_{tot} = -0.91\ \mu_B$ [22] determined with the scaling procedure from the V XMCD, which compares very well with the result from a combined VSM and Fe XMCD study of the identical sample revealing $\mu_{tot} = -1.06\ \mu_B$ [29]. Secondly, we find that the induced moment at the trilayer interface seen for the $Fe/V_2/Fe$ trilayer exhibits an induced moment of $\mu_S^V = 0.57\ \mu_B$ at the interface which is smaller by about a factor of two compared to that for the multilayer. This result is also in good agreement with the calculation by Eriksson *et al* [35] (see table 1). One interpretation of this reduction of the induced V moment for the trilayer in comparison to that for the multilayers is the possible interdiffusion at the Fe/V interface for the multilayered structures occurring because of the higher deposition temperature which is used for the multilayer preparation. The interdiffusion would lead to an apparently larger interface moment for the superlattice, as is also discussed by Eriksson *et al* [35]. Assuming sharp interfaces for multilayers, a long-range spin polarization would then be wrongly concluded. This solves the question concerning the range of the polarization in V with the help of theoretical calculations within an itinerant framework which reproduced the entire XAS and XMCD spectra.

A different approach for the analysis of the early 3d element Cr is discussed in a recent work by Goering *et al* [31]. These authors use the multipole moment analysis presented by van der Laan [32] which is a fitting procedure for the experimental lineshapes within an atomic picture. The application of this procedure to an early 3d element is somewhat surprising, as a large deviation from 2:1 for the branching ratio is determined for Cr also. For those cases it is stated by van der Laan that: 'When in an atomic model the *m*-levels are strongly mixed, the spectral shape will be different and it is possible that the best fit to the data will yield a different value for the spin polarization. In that case it is important to take core-hole interaction implicitly into account' [32]. As presented in our work, we circumvented this difficulty by comparing the data to an experimental standard.

5. Summary

On the basis of the spin–orbit interaction in microscopic materials we have demonstrated that XMCD has its strengths in the element-specific determination of magnetic moments. This allows for the important disentanglement of the magnetism of different elements in layered structures. For interfaces of 5d (W, Ir) and 3d (V) layers with iron, we have demonstrated that the safest procedure is to analyse the integrated XMCD intensity which enters into the sum rules and see whether the integral for the orbital sum rule crosses the zero line or not. For Fe/W we discuss the first experimental case in which a parallel alignment of μ_S and μ_L is found. Theoretically this is an interesting aspect, which has been discussed in the literature

and needs further consideration. For the interface of magnetic and non-magnetic 3d metals, we show for prototype Fe/V/Fe trilayers that basically only at the interface is an antiparallel spin moment at the vanadium site induced. This indicates a short-range spin-polarization. These measurements resolved inconsistencies regarding the range of the polarization predicted by theory and found in earlier experimental works, since interdiffusion at the interfaces in multilayers can lead to an apparent long-range polarization. Furthermore, we demonstrate that the sum rules are not applicable for the early 3d element V because the small spin–orbit splitting between the $2p_{3/2}$ and the $2p_{1/2}$ states leads to strong core-hole correlation effects. Therefore the experimental data are compared to *ab initio* calculations which enabled us to establish a quantitative procedure for determining the ground state properties of V. Vanadium XMCD is interesting in itself, because it cannot be treated as for the classical ferromagnets Fe, Co, and Ni with almost filled 3d bands. Only fully relativistic SP-KKR calculation of the absorption cross-section $\mu(E)$ seems to be adequate for describing the experimental spectra presented here.

Acknowledgments

We want to thank J Minár, D Benea and H Ebert for their KKR calculations of the induced V moments and the corresponding XAS and XMCD spectra. P Poulopoulos, A Ankudinov and J J Rehr are acknowledged for valuable discussions and enlightening ideas. We thank A Rogalev, H C Mertins and F Senf for their technical assistance during the beamtime at the ESRF and BESSY II. The Fe/W and Fe/Ir superlattices were kindly given to us by M Angelakeris and N K Flevaris. This work is supported by BMBF (05 KS1 KEB4), the DFG (Sfb 290) and the ESRF (HE-636).

References

[1] Poulopoulos P and Baberschke K 2001 *Band-Ferromagnetism (Springer Lecture Notes in Physics vol 580)* ed K Baberschke, M Donath and W Nolting (Berlin: Springer) p 283
[2] Thole B T, Carra P, Sette F and van der Laan G 1992 *Phys. Rev. Lett.* **68** 1943
[3] Carra P, Thole B T, Altarelli M and Wang X 1993 *Phys. Rev. Lett.* **70** 694
[4] Chen C T, Idzerda Y U, Lin H-J, Smith N V, Meigs G, Chaban E, Ho G H, Pellegrin E and Sette F 1995 *Phys. Rev. Lett.* **75** 152
[5] Ankudinov A and Rehr J J 1995 *Phys. Rev.* B **51** 1282
[6] Schwitalla J and Ebert H 1998 *Phys. Rev. Lett.* **80** 4586
[7] Ebert H 1996 *Rep. Prog. Phys.* **59** 1665
[8] Ebert H 1996 *Spin–Orbit-Influenced Spectroscopies of Magnetic Solids (Springer Lecture Notes in Physics vol 466)* ed H Ebert and G Schütz (Berlin: Springer) p 159
[9] Wilhelm F, Poulopoulos P, Wende H, Scherz A, Baberschke K, Angelakeris M, Flevaris N K and Rogalev A 2001 *Phys. Rev. Lett.* **87** 207202
[10] Wilhelm F, Poulopoulos P, Ceballos G, Wende H, Baberschke K, Srivastava P, Benea D, Ebert H, Angelakeris M, Flevaris N K, Niarchos D, Rogalev A and Brookes N K 2000 *Phys. Rev. Lett.* **85** 413
[11] Yamada H and Shimizu M 1986 *J. Phys. F: Met. Phys.* **15** L175
[12] Brooks M S S, Eriksson O and Johansson B 1989 *J. Phys.: Condens. Matter* **1** 5861
[13] Ebert H, Zeller R, Drittler B and Dederichs P H 1990 *J. Appl. Phys.* **67** 4576
[14] Hjelm A, Eriksson O and Johansson B 1993 *Phys. Rev. Lett.* **71** 1459
[15] Galanakis I, Alouani M and Dreyssé 2000 *Phys. Rev.* B **62** 3923
[16] Qian X and Hübner W 1999 *Phys. Rev.* B **60** 16192
[17] Qian X and Hübner W 2001 *Phys. Rev.* B **64** 092402
[18] Hübner W 2002 Private communication
[19] Schütz G, Knülle M and Ebert H 1993 *Phys. Scr.* T **49** 302
[20] Tyer R, van der Laan G, Temmerman W M and Szutek Z Private communication
[21] Kornherr C 1997 *Masters Thesis*, University of Munich

[22] Scherz A, Wende H, Baberschke K, Minár J, Benea D and Ebert H 2002 *Phys. Rev.* B **66** 184401
[23] Coehoorn R 1995 *J. Magn. Magn. Mater.* **151** 341
[24] Tomaz M A, Antel W J Jr, O'Brien W L and Harp G R 1997 *J. Phys.: Condens. Matter* **9** L179
[25] Schwickert M M, Coehoorn R, Tomaz M A, Mayo E, Lederman D, O'Brien W L, Lin T and Harp G R 1998 *Phys. Rev.* B **57** 13681
[26] Scherz A, Poulopoulos P, Wende H, Ceballos G, Baberschke K and Wilhelm F 2002 *J. Appl. Phys.* **91** 8760
[27] Lemke L, Wende H, Srivastava P, Chauvistré R, Haack N, Baberschke K, Hunter-Dunn J, Arvanitis D, Mårtensson N, Ankudinov A and Rehr J J 1998 *J. Phys.: Condens. Matter* **10** 1917
[28] Heinz K, Müller S and Hammer L 1999 *J. Phys.: Condens. Matter* **11** 9437
[29] Scherz A, Wende H, Poulopoulos P, Lindner J, Baberschke K, Blomquist P, Wäppling R, Wilhelm F and Brookes N B 2001 *Phys. Rev.* B **64** R180407
[30] Sacchi M, Mirone M, Hague C F, Mariot J-M, Pasquali L, Isberg P and Gullikson E M 1999 *Phys. Rev.* B **60** R12569
[31] Goering E, Bayer A, Gold S, Schütz G, Rabe M, Rüdiger U and Güntherodt G 2002 *Phys. Rev. Lett.* **88** 207203
[32] van der Laan G 1997 *Phys. Rev.* B **55** 8086
[33] Lindner J and Baberschke K 2003 *J. Phys.: Condens. Matter* **15** S465
[34] Pelzl J, Meckenstock R, Spoddig D, Schreiber F, Pflaum J and Frait Z 2003 *J. Phys.: Condens. Matter* **15** S451
[35] Eriksson O, Bergqvist L, Holmström E, Bergman A, LeBacq O, Frota-Pessoa S, Hjörvarsson B and Nordström L 2003 *J. Phys.: Condens. Matter* **15** S603